10568 *Biochemistry* **2009,** *48,* 10568–10576
DOI: 10.1021/bi900608m

BIOCHEMISTRY
including biophysical chemistry & molecular biology
Article

Annexin A5 Directly Interacts with Amyloidogenic Proteins and Reduces Their Toxicity†

Sahar Bedrood,‡ Sajith Jayasinghe,§ Derek Sieburth,∥ Min Chen,∥ Saskia Erbel,⊥ Peter C. Butler,@ Ralf Langen,*,‡ and Robert A. Ritzel*,⊥,@

‡*Department of Biochemistry and Molecular Biology, Zilkha Neurogenetic Institute, Keck School of Medicine, University of Southern California, Los Angeles, California 90033,* §*Department of Chemistry and Biochemistry, California State University, San Marcos, California 92096,* ∥*Department of Cell and Neurobiology, Zilkha Neurogenetic Institute, Keck School of Medicine, University of Southern California, Los Angeles, California 90033,* ⊥*Department of Internal Medicine I and Clinical Chemistry, University of Heidelberg, 69120 Heidelberg, Germany, and* @*Larry Hillblom Islet Research Center, UCLA David Geffen School of Medicine, Los Angeles, California 90095-7073*

Received April 8, 2009; Revised Manuscript Received October 2, 2009

ABSTRACT: Protein misfolding is a central mechanism for the development of neurodegenerative diseases and type 2 diabetes mellitus. The accumulation of misfolded α-synuclein protein inclusions in the Lewy bodies of Parkinson's disease is thought to play a key role in pathogenesis and disease progression. Similarly, the misfolding of the *β*-cell hormone human islet amyloid polypeptide (h-IAPP) into toxic oligomers plays a central role in the induction of *β*-cell apoptosis in the context of type 2 diabetes. In this study, we show that annexin A5 plays a role in interacting with and reducing the toxicity of the amyloidogenic proteins, h-IAPP and α-synuclein. We find that annexin A5 is coexpressed in human *β*-cells and that exogenous annexin A5 reduces the level of h-IAPP-induced apoptosis in human islets by ∼50% and in rodent *β*-cells by ∼90%. Experiments with transgenic expression of α-synuclein in *Caenorhabditis elegans* show that annexin A5 reduces α-synuclein inclusions in vivo. Using thioflavin T fluorescence, electron microscopy, and electron paramagnetic resonance, we provide evidence that substoichiometric amounts of annexin A5 inhibit h-IAPP and α-synuclein misfolding and fibril formation. We conclude that annexin A5 might act as a molecular safeguard against the formation of toxic amyloid aggregates.

Protein misfolding and the deposition of amyloid fibrils are hallmarks of many diseases, including Alzheimer's disease (amyloid *β*-protein), Parkinson's disease (α-synuclein), Huntington's disease (huntingtin), and type 2 diabetes [islet amyloid polypeptide (IAPP)][1] (*1*−*8*). Although different polypeptides with little or no sequence similarity form fibrils in the various diseases, there are a number of structural similarities with respect to the mechanism of misfolding as well as the toxicity of the misfolded proteins. In vitro studies have shown that amyloid fibril formation is a stepwise process, in which nonfibrillar oligomeric structures are formed before the first fibrils can be detected (*1*, *9*). Although the pathology of amyloid diseases is dominated by an abundance of fibrillar deposits, the nonfibrillar oligomers have begun to receive much attention, as they are now thought to represent the primary toxic species (*1*, *4*, *7*, *10*). In fact, some diseases are characterized by proteinaceous deposits in which nonfibrillar amyloid oligomers rather than amyloid fibrils represent the primarily deposited material. An example of such a disease is macular degeneration (*11*). In the endocrine pancreas of humans with type 2 diabetes, the *β*-cell peptide, IAPP, misfolds and aggregates into islet amyloid (*12*, *13*) and is thought to promote *β*-cell apoptosis in type 2 diabetes (*14*−*16*). The propensity for human IAPP (h-IAPP) to induce apoptosis has been described in different experimental models, including *β*-cell and non-*β*-cell lines (*17*−*21*), human islets (*10*, *17*, *21*), and transgenic animal models (*16*, *22*, *23*). The Lewy bodies occurring in Parkinson's disease are intracytoplasmatic inclusion bodies and are characterized by an abundance of misfolded α-synuclein protein (*24*, *25*), which is thought to be the primary toxic principle leading to the degeneration of dopaminergic neurons. As in the case of other amyloidogenic peptides, the detailed mechanism of toxicity is unclear, but destabilization of cellular metabolism by pronounced membrane permeabilization is likely to play an important role (*1*, *6*, *9*, *26*).

Annexins represent a highly conserved family of Ca^{2+}-dependent membrane-binding proteins. They are abundantly expressed in a wide range of tissues (*27*, *28*) and found in intra- and extracellular locations (*29*, *30*). Annexin A5 (*31*) has been shown to offer protection from the cytotoxicity of Alzheimer's *β*-protein (A*β*), and it was proposed that this occurs by competitive interaction at membrane phosphatidylserine (*32*). Recently, it was reported that the aggregated extracellular deposits (drusen) of subjects with age-related macular degeneration contain annexin A5 (*33*). Thus, annexin A5 is codeposited with misfolded proteins in some disease states. To shed further light on annexin A5's potential role in preventing and/or reversing the toxic

†These studies were funded in part by the National Institutes of Health (Grants GM063915 and AG027936 to R.L. and Grant DK 61539 to P.C.B.), by the American Parkinson Disease Association and the Baxter Foundation (to D.S.), and by the Deutsche Forschungsgemeinschaft (DFG Ri 1055/3-1) and the German Diabetes Association (to R.A.R.).

*To whom correspondence should be addressed. R.A.R.: Department of Internal Medicine I and Clinical Chemistry, University of Heidelberg, Im Neuenheimer Feld 410, 69120 Heidelberg, Germany; telephone, +49-6221-568601; fax, +49-6221-564233; e-mail, Robert.Ritzel@med.uni-heidelberg.de. R.L.: Department of Biochemistry and Molecular Biology, Zilkha Neurogenetic Institute, University of Southern California, 1501 San Pablo St., Los Angeles, CA 90033; telephone, (323) 442-1323; fax, (323) 442-4404; e-mail, langen@usc.edu.

[1]Abbreviations: IAPP, islet amyloid polypeptide; h-IAPP, human islet amyloid polypeptide; ThT, thioflavin T; EPR, electron paramagnetic resonance; SEM, standard error of the mean.

 Published on Web 10/08/2009

actions of amyloidogenic proteins, we hypothesized that annexin A5 may directly inhibit the misfolding of amyloidogenic proteins. Specifically, we posed the question of whether annexin A5 can modulate the misfolding of IAPP and α-synuclein in vitro and offer protection from aggregation and toxicity in vivo.

MATERIALS AND METHODS

Human Islet Tissue. Human pancreatic islets for static incubation experiments were isolated from the pancreas retrieved from three nondiabetic, heart-beating organ donors by the Diabetes Institute for Immunology and Transplantation, University of Minnesota, Minneapolis, MN (B. J. Hering), and the Northwest Tissue Center, Seattle, WA (R. P. Robertson). Approval to use islets for research purposes was given by the local ethics committees at both institutions. The islets were maintained in RPMI culture medium at 5 mM glucose and 37 °C in humidified air containing 5% CO_2. After the islet isolation process, the islets were cultured for 3−5 days before experiments were performed. Aliquots of human islets were incubated for 48 h with vehicle (H_2O and 0.5% acetic acid), 40 μM rat IAPP, 40 μM h-IAPP, and 40 μM h-IAPP with 1 μM annexin A5. After static incubation, the number of apoptotic cells in human islets was detected using the TUNEL staining method (In Situ Cell Death Detection Kit, AP, Roche Diagnostics, Indianapolis, IN). Tissue samples were analyzed on an inverted microscope (Inverted System Microscope IX 70, Olympus, Melville, NY) as described previously (*21*).

Annexin A5. For the experiments presented here, annexin A5 was originally expressed in *Escherichia coli* by Schlaepfer and colleagues (*34*) and then subcloned into the pSE420 plasmid (Invitrogen, Carlsbad, CA) via a NcoI and HindIII site in the vector and cDNA (*35*). The recombinant annexin A5 was purified by reversible Ca^{2+} binding to phospholipid vesicles followed by column chromatography. Concentrations were determined from A_{280} using an extinction coefficient of 21000 M^{-1}. The purity of annexin A5 was determined using mass spectrometry and sodium dodecyl sulfate (SDS) gel electrophoresis (data not shown).

Time-Lapse Video Microscopy (*TLVM*). RIN cells (a gift from C. J. Rhodes), a rodent β-cell line, were maintained in culture in Click's culture medium with 10 mmol/L glucose and 10% FBS at 37 °C in humidified air containing 5% CO_2. After trypsin digestion of the primary cell culture, aliquots of suspended cells were placed in a specially prepared microculture dish (2.3 cm diameter, ΔT Culture Dish, Bioptechs, Butler, PA) and kept in a conventional incubator (model 3110, Forma Scientific, Marietta, OH) over the following 24 h. TLVM was then performed as previously described (*21*). Briefly, the microculture dish was removed from the incubator and mounted onto the motorized stage (H107, ProScan, Prior Scientific) of an inverted microscope (Inverted System Microscope IX 70). The temperature inside the dish was dynamically kept at 37 ± 0.1 °C (ΔT Culture Dish Controller). For time-lapse experiments, images of selected fields were acquired with an analogue camera (3-CCD camera, Optronics) every 10 min, stored, and analyzed on a personal computer.

Confocal Microscopy. Human pancreatic islets for confocal microscopy were provided by the Cell Isolation and Transplantation Center at the University of Geneva School of Medicine (Geneva, Switzerland). Approval to use islets for research purposes was given by the local ethics committee. Islets were washed with PBS and fixed in 4% paraformaldehyde at 4 °C overnight. The next day, islets were washed twice with PBS and embedded in 2% agarose, dehydrated in 70% ethanol, and embedded in paraffin. Sections (3 μm) were cut from paraffin blocks (Mikrotom Leica RM 2165, Wetzlar, Germany) for subsequent analysis by immunofluorescence. Paraffin sections of islets were stained for annexin A5 (antibody from Santa Cruz, Heidelberg, Germany) (1:200 dilution) and human amylin (antibody from Santa Cruz) (1:50 dilution). Sections were deparaffinized and rehydrated followed by permeabilization with 0.4% Triton X-100 and PBS for 10 min. After being blocked (3% BSA and 0.2% Triton X-100 and PBS) for 1 h, sections were incubated with the indicated primary antibody in a wet chamber at 4 °C overnight. Immunostaining was visualized by using fluorescein or rhodamine-conjugated secondary antibodies (1:50 dilution; Jackson ImmunoResearch, West Grove, PA). After the nuclei had been stained with bisbenzimide H 33258 (Sigma, Taufkirchen, Germany), slides were mounted with Vectashield mounting medium (Vector Laboratories, Burlingame, CA) and placed under cover slips. Human islet cell morphology was determined by confocal microscopy using a Perkin Elmer spinning disc confocal ERS-FRET instrument on a Nikon TE2000 inverted microscope in the Nikon Imaging Center at the University of Heidelberg.

IAPP Stock Solutions. Human and rat IAPP were purchased from Bachem (Torrance, CA). For the preparation of stock solutions, the lyophilized peptides were reconstituted with deionized water containing 0.5% acetic acid. Human IAPP was prepared as in previous preparations that gave rise to toxic species (*1*, *21*). Briefly, cell culture experiments were conducted by dilution of stock solutions with the culture medium to yield a final concentration of 40 μM and then directly applied to the cells. Acetic acid concentrations in the culture medium applied to cells were always $< 0.003\%$.

Electron Paramagnetic Resonance (*EPR*) *and Site-Directed Spin Labeling*. Spin-labeled IAPP was prepared as described previously (*36*). Briefly, h-IAPP containing single cysteines at either position 14 or 21 was obtained from Biomer Technology (Hayward, CA). Mutant h-IAPP was labeled with a 3-fold excess of MTSL label [1-oxyl-2,2,5,5-tetramethyl-Δ3-pyrroline-3-methyl methanethiosulfonate, obtained from Toronto Research Chemicals (Toronto, ON)] for 1 h at room temperature. Labeled peptide was recovered via cation exchange chromatography and desalted with a C-18 silica column (Macro Spin Column, Havard Biosciences, Holliston, MA). The spin-labeled Cys residue generated under these conditions is termed R1. Spin-labeled h-IAPP was collected and stored in hexafluoro-2-propanol (HFIP). Prior to usage, HFIP was evaporated and the sample was dissolved in 10 mM phosphate, 100 mM NaCl (pH 7) buffer to a final concentration of 100 μM. For α-synuclein, a truncated mutant (115ter α-synuclein) of recombinant human α-synuclein containing residues 1−115 was generated via addition of two stop codons between residues 115 and 116. The wild-type α-synuclein construct (in pRK172) and purification methods were described in a previous protocol (*37*). The 115ter α-synuclein was then filtered through an Amicon YM-100 spin filter (MWCO 1 × 105, Millipore) to remove any pre-aggregates. Immediately before spin labeling was conducted, dithiothreitol was removed by loading the protein solution onto a PD-10 column (Amersham Biosciences, GE Healthcare) equilibrated with buffer containing 20 mM Hepes (pH 7.4), 100 mM NaCl, and 1 mM EDTA and then eluted using the same buffer. The 115ter α-synuclein was labeled with a 10-fold molar excess of R1 MTSL spin-label

1-oxyl-2,2,5,5-tetramethyl-Δ3-pyrroline-3-methyl methanethiosulfonate (Toronto Research Chemicals) for 1 h at room temperature. Excess label was removed using PD-10 columns with the aforementioned elution buffer. Spin-labeled proteins were washed twice with elution buffer, concentrated using Amicon Ultra-4 centrifugal filter units (MWCO 5 × 103, Millipore), and assembled into fibrils as described previously (*38*).

To evaluate the effect of annexin A5 on h-IAPP and 115ter α-synuclein fibril formation, 100 μM spin-labeled h-IAPP and 115ter α-synuclein were incubated at room temperature (for h-IAPP) and at 37 °C under constant agitation (for 115ter α-synuclein samples) for 3−5 days in the absence or presence of annexin A5 (20 μM). Fibrils and aggregates were harvested by centrifugation (13000 rpm for 10 min using a model 5415D Eppendorf tabletop centrifuge) and washed with buffer. For EPR spectroscopy, samples were loaded into glass capillary tubes (0.6 mm inner diameter and 0.84 outer diameter, VitroCom, Mt. Lakes, NJ). Spectra were obtained on a Bruker EMX spectrometer (Bruker Instruments, Billerica, MA) at room temperature at an incident microwave power of 12 mW with a scan range of 150 G.

Electron Microscopy. To examine the effect of annexin A5 on fibril growth, 100 μM amyloid-forming peptides (wt h-IAPP or 115ter α-synuclein) were incubated with and without annexin A5 for 4 days as described above. After the incubation period, 10 μL of the samples was adsorbed onto carbon and formavar-coated copper grids and negatively stained with a 2% (w/v) uranyl acetate solution for 5 min. The stained grids were examined and photographed using a JEOL JEM-1400 electron microscope at 80−100 kV.

Thioflavin T Fluorescence Assay. The fibrillization process of h-IAPP and 115ter α-synuclein was monitored using the fluorescence increase of thioflavin T (ThT), a dye known to preferentially bind amyloid fibrils. ThT fluorescence increases in a solution of freshly reconstituted peptide as amyloid fibrils grow. For the h-IAPP thioflavin T assay, wt h-IAPP was reconstituted in 6 M guanidine hydrochloride buffer (150 μL per 0.5 mg of h-IAPP) and loaded into a hydrated (with deionized water) C-18 silica column (Macro Spin Column, Havard Biosciences). Guanidine was washed out with 150 μL of deionized water. Then h-IAPP was recovered from the column by application of 150 μL of hexafluoro-2-propanol (HFIP). The HFIP in the flow-through was allowed to evaporate, and the remaining peptide was reconstituted with deionized water containing 0.5% acetic acid and 2.5% HFIP. In the case of α-synuclein, 100 μM 115ter α-synuclein was incubated with 20 μM annexin A5. A 5 μM ThT aliquot in glycine buffer (50 mM) was added to each of the samples, and real-time emission intensities were measured at 482 nm with excitation at 450 nm. Measurements were performed at room temperature with excitation and emission slit widths of 1 and 10 nm, respectively. Fluorescence measurements were taken using a Jasco FP-6500 spectrofluorometer. Plots of ThT emission intensity as a function of time were fitted to a sigmoidal curve (nonlinear regression analysis).

Transgenic Caenorhabditis elegans Strains. To make the annexin A5 expression construct, a PCR-amplified full-length human annexin A5 cDNA fragment was subcloned into NheI and KpnI sites of expression vector pPD40.26 (gift of A. Fire) containing the *myo-3* promoter. The *vjEx171* and *vjEx172* arrays were generated by co-injecting this annexin A5 expression construct (25 ng/μL) together with the injection marker KP# (40 ng/μL) into a Punc-54::synuclein::YFP-expressing strain of *C. elegans* NL5901 (a gift of E. Nollen). These arrays were subsequently crossed into a punc-54::YFP UA52 strain (gift of G. Caldwell). Young adult animals were paralyzed using sodium azide and mounted on 2% agarose pads for imaging. Images were acquired on a Nikon 90i microscope using a Nikon Plan Apo 60× objective (NA = 1.4) and a Coolsnap ES2 (Photometrics) camera controlled with Metamorph (Universal Imaging/Molecular Devices). Body wall muscles in the pharynx were imaged from ∼30 laterally oriented animals per genotype. A maximum intensity projection was obtained from image stacks of muscles. Images were thresholded in Metamorph, and the number of puncta above threshold (determined by background muscle fluorescence) was counted.

Western Blotting. Western blotting was performed to determine if annexin A5 protein expression in *C. elegans* alters the expression of α-synuclein. For Western analysis, 400 washed adult worms were Downs homogenized in 150 μL of worm lysis buffer [50 mM Tris (pH 7.5), 10% glycerol, 150 mM NaCl, and a protease inhibitor tablet (Roche Diagnostics)] and centrifuged at 15000*g* for 1 min. The total protein in the supernatant was subjected to a protein assay using the BCA kit (Thermo Fisher Scientific). Samples were diluted in sample buffer containing 1% SDS, and 1 μg of protein was subjected to Western blot analysis. Protein (1 μg/μL) was separated via 12% SDS−PAGE and transferred to PVDF membranes (Bio-Rad, Hercules, CA). Membranes were blocked with 10% nonfat dry milk in 0.1% Tween/Tris-buffered saline (TBS-T) and incubated with TBS-T containing polyclonal rabbit anti-α-synuclein antibody (1:1000) (Chemicon International, Temecula, CA) and monoclonal mouse anti-actin antibody (Calbiochem, Darmstadt, Germany). Membranes were washed five times with TBS-T and incubated with horseradish peroxidase-conjugated goat anti-rabbit IgG (1:3000) (Zymed Laboratories, South San Francisco, CA) and sheep anti-mouse IgG (Amersham) for 1 h. Proteins were visualized using enhanced chemiluminescence (ECL) (Amersham).

To assess if the presence of the annexin A5 transgene alters the expression of YFP, whole-worm lysates of *vjEx171* arrays in UA52 animals were subjected to a radio immunoprecipitation assay to extract total protein. Total protein lysate was separated via 12% SDS−PAGE and transferred to PVDF membranes (Bio-Rad). Membranes were blocked with 10% nonfat dry milk in 0.1% Tween/Tris-buffered saline (TBS-T) and incubated with TBS-T containing monoclonal anti-GFP antibody (which cross reacts with YFP, 1:1000) (Invitrogen, Inc.) or actin antibody. Membranes were washed five times with TBS-T and incubated with horseradish peroxidase-conjugated sheep anti-mouse IgG (Amersham) for 1 h. Proteins were visualized using enhanced chemiluminescence (Amersham).

Calculations and Statistical Analysis. The best-fit curves of the amyloid protein-induced change in relative fluorescence intensity in relationship to annexin A5 concentration in thioflavin T time-dependent normalized fluorescence intensity were derived by nonlinear regression analysis.

Differences in the number of apoptotic cells per islet or percentage of apoptotic RIN cells were analyzed by ANOVA and Tukey's multiple-comparison test. A probability of a $< 5\%$ occurrence by chance alone denoted statistical significance.

RESULTS

Annexin A5 Protects Human Islet Tissue and β-Cells from h-IAPP Toxicity. Static incubation of human islets with freshly reconstituted h-IAPP for 48 h resulted in a 4-fold increase

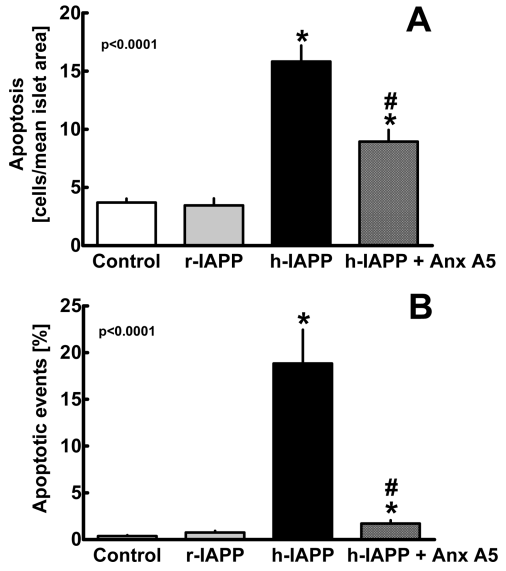

FIGURE 1: (A) Mean number of apoptotic cells in human islets (n = 3 donors, 7−9 experiments per group, total islet number per group 61−97) after incubation for 48 h with vehicle (control), rat IAPP (40 μM), h-IAPP (40 μM), or h-IAPP (40 μM) with annexin A5 (1 μM). (B) Percentage of apoptotic RIN cells during a 24 h incubation (time-lapse microscopy) with vehicle (control), rat IAPP (40 μM), h-IAPP (40 μM), or h-IAPP (40 μM) with annexin A5 (1 μM). Data ± SEM. P-value derived by ANOVA. Group comparisons by *: $p < 0.05$ versus control. #: $p < 0.05$ versus h-IAPP.

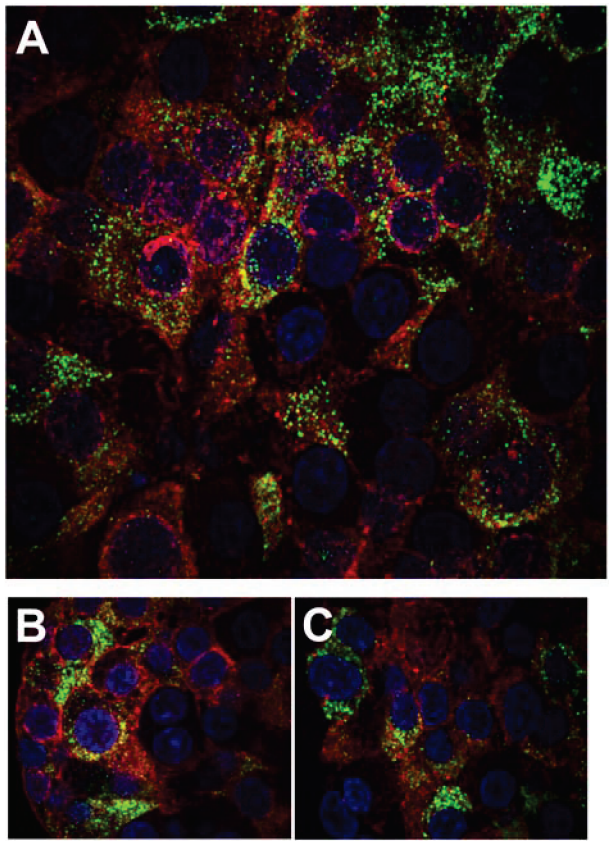

FIGURE 2: Spinning-disc confocal microscopic images of 3 μM sections of three isolated human islets from two nondiabetic organ donors. Immunostaining was performed for annexin A5 (red), human IAPP (green), and nuclei with DAPI (blue). (A) Three-dimensional reconstruction of the full section. (B and C) Single-plane images. Annexin A5 is present in β- and non-β-cells in human islets. Magnification of 1000×.

in the number of apoptotic cells compared to incubation with vehicle (control) or non-amyloidogenic rat IAPP (Figure 1A). Annexin A5 reduced the number of apoptotic cells in human islets after incubation for 48 h by ~50%, demonstrating that annexin A5 has a protective effect with regard to h-IAPP toxicity. In RIN cells, incubation with h-IAPP also leads to an induction of apoptosis (Figure 1B). Annexin A5 leads to an ~90% reduction in the level of h-IAPP-induced apoptosis. For such protection to be physiologically relevant, it is essential to know that annexin A5 is present in human β-cells in which h-IAPP is expressed. To test this, we performed confocal microscopy of human islet sections from two nondiabetic tissue donors. As shown in Figure 2, there are numerous examples of islet cells being costained for h-IAPP (β-cells) and annexin A5. These data show that annexin A5 is present in human β-cells.

Annexin A5 Reduces Thioflavin T Fluorescence and the Level of Fibril Formation (as judged by EM) of h-IAPP and α-Synuclein. To test whether annexin A5 might directly affect misfolding of amyloidogenic proteins such as h-IAPP or α-synuclein in vitro, we performed in vitro assays using ThT fluorescence, electron microscopy, and EPR spectroscopy.

The ThT assay is based upon the fluorescence enhancement that occurs when amyloidogenic peptides or proteins undergo a conformational reorganization into fibrils and other oligomers. Consistent with previous reports (*39*), the time-dependent kinetics of h-IAPP and α-synuclein fibril formation followed a sigmoidal pattern (Figure 3A,B). The fibril formation for α-synuclein is more rapid than what is typically seen for the wild-type protein, because we employed the highly amyloidogenic 115ter truncation mutant (*37*). This mutant contains the entire amyloidogenic core region and gives structurally indistinguishable aggregates but aggregates more avidly and reproducibly than the wild-type protein (*37*). With annexin A5, the time-dependent increase in thioflavin T fluorescence is largely prevented, indicating that annexin A5 directly interacts with h-IAPP and 115ter α-synuclein and prevents the formation of thioflavin positive fibrils. These findings were further supported by electron microscopy, which indicated that annexin A5 resulted in formation of predominately amorphous aggregates rather than fibrils (Figure 3C−F).

Site-Directed Spin Labeling and EPR Spectroscopy Reveal That h-IAPP and α-Synuclein Fibril Formation Is Strongly Altered in the Presence of Annexin A5. To further investigate the notion that annexin A5 has a direct impact on amyloid misfolding and fibril formation, we employed site-directed spin labeling and EPR spectroscopy. Using this approach, we had previously shown that h-IAPP fibrils (*36*), like those from many other amyloidogenic proteins (*37*, *38*, *40*−*42*), form a parallel, in-register structure in which the same residues are stacked on top of each other. Because of the proximity of the same sites in fibrils, fibrils of spin-labeled h-IAPP derivatives give rise to highly characteristic EPR spectra (*42*). As shown with two representative examples in Figure 4, the EPR spectra of fibrils grown from h-IAPP (21R1) and 115ter α-synuclein (52R1) have strong components of exchange narrowing and dipolar broadening, both of which result from the proximity of the same residues. To test whether annexin A5 can interfere with the formation of these specific structures, we repeated the aforementioned experiments in the presence of substoichiometric amounts of annexin A5. The EPR spectra of the aggregates that formed in the presence of annexin A5 were strikingly altered and characterized

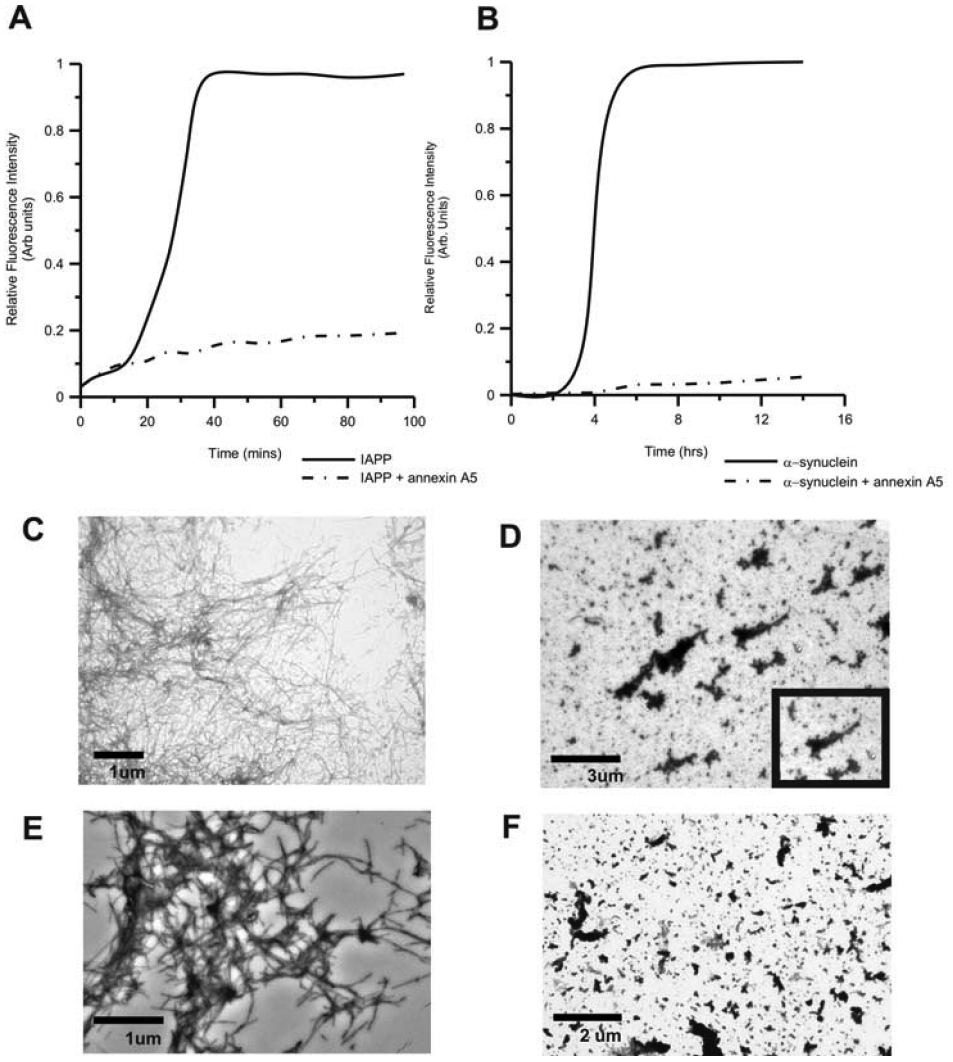

FIGURE 3: Thioflavin T curves and EM images of amyloid fibrils with and without annexin A5. (A) Time-dependent normalized ThT emission curves of h-IAPP (20 μM) with (dashed line) and without (solid line) annexin A5 (4 μM). The solid and dashed lines are derived by nonlinear regression analysis of three (*n*) experiments per group. (B) Time-dependent normalized ThT emission curves of 115ter α-synuclein (100 μM) with (solid line) and without annexin A5 (20 μM) (dashed line). The ThT curves are normalized to the maximal observed intensity at the end of each aggregation reaction. Panels C and E show EM images of 100 μM h-IAPP (3000× magnification) and 115ter α-synuclein (6000× magnification) fibrils, respectively, grown in the absence of annexin A5. Panels D and F show h- IAPP (4000× magnification) and 115ter α-synuclein (2000× magnification) with annexin A5 in a 3:1 ratio. Amorphous protein aggregates and no fibrils are seen throughout the sample when amyloidogenic proteins are observed in the presence of annexin A5. The inset shows a 15000× magnification to illustrate the absence of fibrils at higher magnifications.

by a loss of the pronounced spin−spin interaction, further illustrating that annexin A5 alters the misfolding.

It should be noted that the EM, ThT, and EPR experiments all used substoichiometric amounts of annexin A5. Thus, annexin A5 cannot merely act by binding to all available monomeric amyloidogenic proteins. In fact, we found no detectable EPR spectral changes when equimolar amounts of annexin A5 were mixed with freshly prepared, predominantly monomeric, spin-labeled h-IAPP (data not shown). On the basis of these data, it is likely that annexin A5 alters misfolding by interacting with misfolded subpopulations of the respective amyloidogenic proteins that are on the aggregation pathway.

Annexin A5 Expression Reduces the Number of α-Synuclein Inclusions in Vivo. Having established that annexin A5 can alter misfolding in vitro and protect proteins from toxicity when added together exogenously with the amyloidogenic peptide, we next asked whether annexin A5 might also affect the misfolding when co-expressed endogenously in the presence of a cytosolic amyloidogenic protein, such as α-synuclein. Toward this end, we chose *C. elegans* as a model system. Previous work has shown that α-synuclein inclusions can be conveniently visualized in *C. elegans* body wall muscles as fluorescent puncta in animals expressing α-synuclein−YFP fusion proteins (α-synuclein::YFP) (*43*, *44*). Thus, we expressed full-length human annexin A5 cDNA in body wall muscles (using the *myo-3* promoter) in animals overexpressing synuclein::YFP (under the *unc-54* promoter) (*44*) and compared the number of inclusions to the number in control animals that were not expressing annexin A5. We quantified the number of fluorescent puncta in muscles in the head region that were brighter than background muscle fluorescence. We found that muscles of animals expressing annexin A5 had a reduced number of fluorescent puncta compared to nontransgenic controls (Figure 5). This effect is consistent with a reduction in the level of formation of inclusions by annexin A5 but could potentially be due to lower α-synuclein protein levels in muscles. Thus, we examined the abundance of

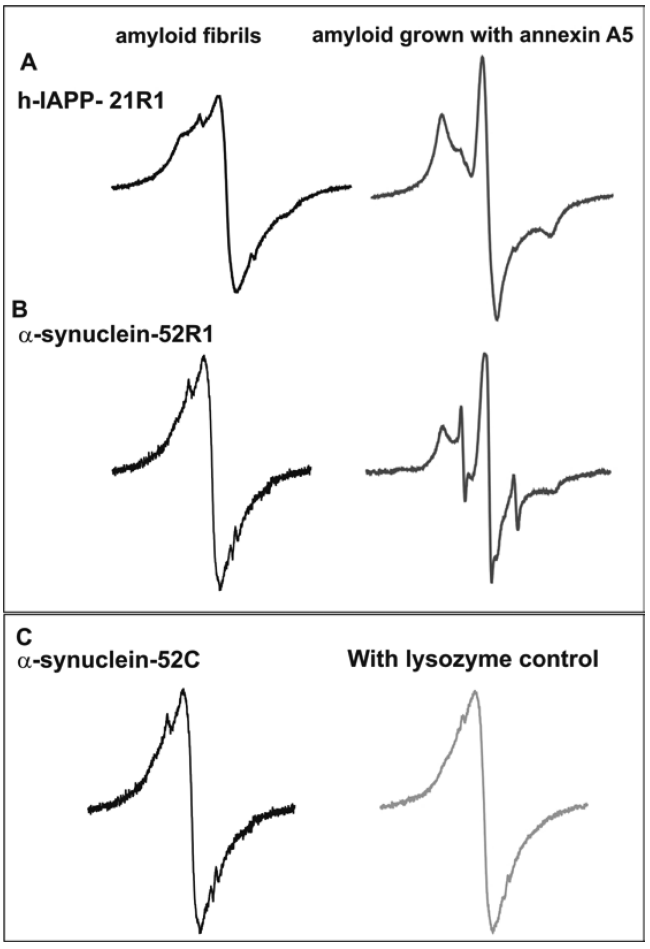

FIGURE 4: EPR spectra of R1-labeled h-IAPP and 115ter α-synuclein in the presence of annexin A5. To assess the effect of annexin A5 on amyloid misfolding, 20 μM annexin A5 was added to 100 μM spin-labeled (A) h-IAPP (21R1) or (B) 115ter α-synuclein (52R1) peptide and allowed to form fibrils. The black spectra are for control amyloid fibrils grown in the absence of annexin A5, and the gray spectra are for amyloid fibrils grown in the presence of annexin A5. A sample of 115ter α-synuclein was incubated with lysozyme (C) to control for structural effects caused by the presence of any large protein. All spectra were normalized to the same number of spins.

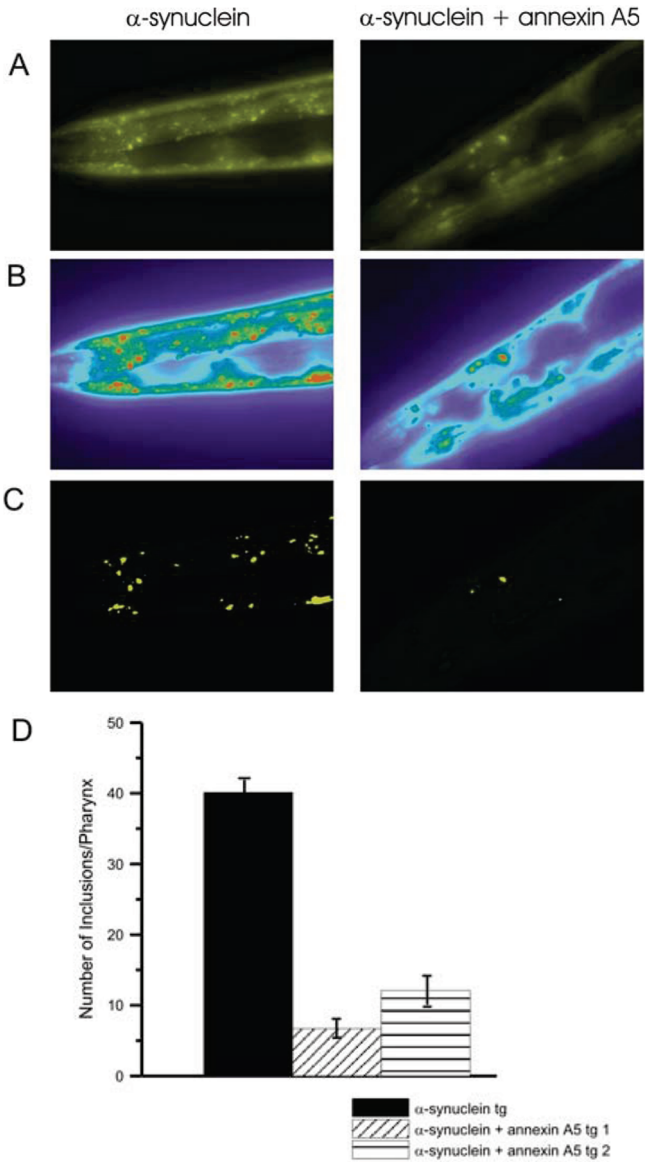

FIGURE 5: Annexin A5 expression decreases the number of α-synuclein inclusions in vivo. (A) Representative fluorescent images of head muscles of transgenic young adult animals expressing either α-synuclein::YFP alone (the pkIs2386 transgene) or α-synuclein::YFP with human annexin A5 (pkIs2386; vjEx137). (B) False colored images from panel A with red and purple representing the highest and lowest pixel intensities, respectively. (C) Thresholded images from panel A showing pixel intensities above background in green. (D) Quantification of the number of inclusions above threshold per pharynx averaged over 20 animals. Data from two independently generated transgenic lines expressing annexin A5 are shown. The standard error is shown ($p < 0.001$).

synuclein::YFP in animals expressing annexin A5 compared to controls. We found no change in normalized synuclein::YFP protein levels in whole animal lysates (Figure 6A,B). To test whether annexin A5 alters gene expression of α-synuclein from this transgene, we examined if annexin A5 expression could alter the abundance of another protein, YFP, expressed under the same promoter used to drive α-synuclein expression. We found no change in YFP abundance in whole animal lysates from annexin A5-expressing animals compared to controls (Figure 6C, D), confirming that annexin A5 does not alter gene expression of the α-synuclein transgene. Thus, the reduction in the number of fluorescent puncta is not a consequence of a reduced level of α-synuclein expression but is consistent with the ability of annexin A5 to directly affect α-synuclein misfolding.

DISCUSSION

In this study, we show that annexin A5 protects cultured human islet tissue and β-cells by attenuating h-IAPP-induced apoptosis. Consistent with these results, we found that annexin A5 also reduces the number of inclusions of α-synuclein in an in vivo model (*C. elegans*) of α-synuclein aggregation. Several lines of evidence show that annexin A5, in addition to its well-known ability to interact with lipids (e.g., membrane phosphatidylserine) and thereby potentially indirectly affecting misfolding and toxicity (*32*), directly interferes with the aggregation and misfolding of h-IAPP and α-synuclein. First, annexin A5 alters h-IAPP and 115ter α-synuclein misfolding as judged by thioflavin fluorescence, electron microscopy, and EPR spectroscopy. Second, only substoichiometric amounts of annexin A5 are required to attenuate the pro-apoptotic effects of h-IAPP, suggesting that interaction of annexin A5 with a subset of h-IAPP molecules is sufficient to exert these effects. Third, the EPR and electron microscopy data show that the interaction of annexin A5 with h-IAPP and

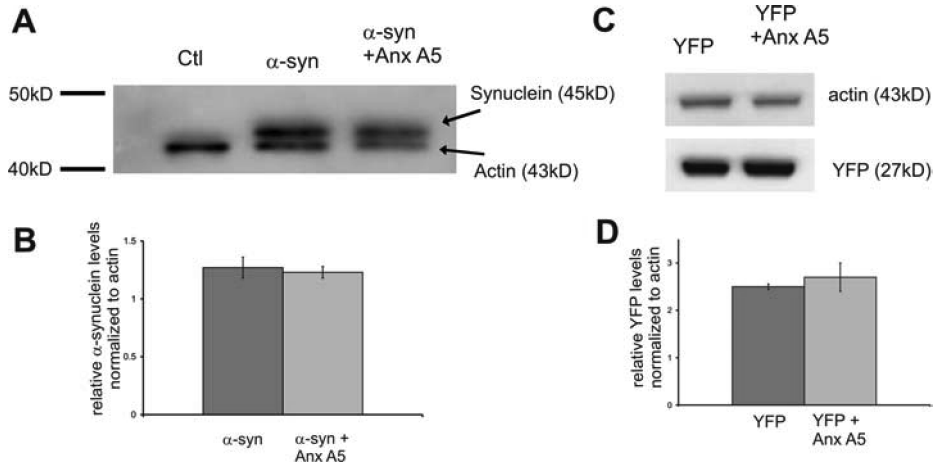

FIGURE 6: Expression of α-synuclein in annexin A5 transgenic *C. elegans*. (A) Immunoblots of total protein extracts from control animals containing no α-synuclein or annexin A5 (lane 1), α-synuclein transgene (lane 2), and α-synuclein with the annexin A5 transgene (lane 3). The samples were subjected to SDS−PAGE and Western blotting with anti-α-synuclein and anti-actin antibodies to detect whether the annexin A5 transgene alters the expression of α-synuclein. Actin (43 kDa) was used as a control. (B) α-Synuclein protein levels in animals with and without the annexin A5 transgene. (C) Immunoblot of total protein extracts from animals containing YFP only (lane 1) and YFP with annexin A5 (lane 2). The samples were subjected to SDS−PAGE and Western blotting with anti-YFP and anti-actin antibodies to detect whether the annexin A5 transgene alters the expression of YFP. (D) YFP protein levels in animals with and without the annexin A5 transgene.

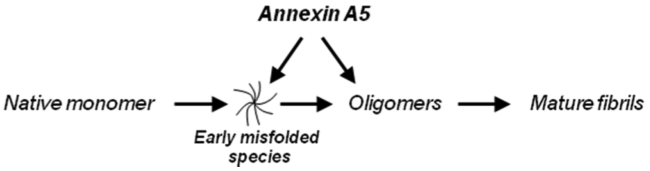

FIGURE 7: Model explaining the mechanism of annexin A5 action. Annexin A5 alters misfolding and interferes with fibril formation. This effect is caused by interaction with a subset of molecules, which are generated during the misfolding process rather than a direct interaction with the bulk monomer. The precise nature of the species with which annexin A5 interacts is not yet known, but it is likely that they represent misfolded species that are directly on the pathway to fibril formation.

α-synuclein molecules alters the aggregation pathway and inhibits the formation of the typical h-IAPP and α-synuclein fibrils. Thus, annexin A5 is likely to interact with a subset of h-IAPP and α-synuclein molecules that are in a pathogenic conformation and/or on the pathway toward fibril formation. Since these results were found using two amyloidogenic proteins, we hypothesize that annexin A5 plays a more generalized protective role for amyloid proteins (Figure 7).

Our cell culture and animal model studies show that annexin A5 can affect misfolding either when added exogenously or when expressed endogenously. Annexin A5 has been reported to be present primarily intracellularly but also extracellularly (*29*, *30*). Since IAPP is synthesized in β-cells and then stored in the secretory vesicles, there probably is little intracellular interaction between these molecules in a nondiabetic environment. In the context of type 2 diabetes, an interaction of annexin A5 with h-IAPP might occur outside (after exocytosis) as well as inside β-cells (damaged vesicle membranes by aggregating h-IAPP). These experiments do not resolve this issue. However, in the experiments with isolated human islets and β-cells in culture presented here, it is likely that the extracellular presence of annexin A5 directly prevented the formation of toxic protofibrillar species of applied h-IAPP. The data on annexin A5 concentrations in human cells are sparse, but the concentrations applied to human islets in culture in these experiments (1 μM) roughly correspond to those found intracellularly (*29*, *45*). Lower concentrations might be expected in the extracellular environment.

Animal models with transgenic expression of h-IAPP develop a phenotype with islet amyloid, β-cell loss due to an increased level of apoptosis and impaired β-cell function similar to those of human type 2 diabetes (*16*, *46*). The initial aggregation and formation of toxic h-IAPP oligomers occur intracellularly (*23*, *47*, *48*), corresponding to the location of high annexin A5 concentrations. It is, therefore, quite likely that intracellular annexin A5 could directly interact with and alter the misfolding of intracellular h-IAPP. This hypothesis should be directly tested in future studies. The in vivo experiments with *C. elegans* provide direct experimental evidence that annexin A5 is indeed effective also in the intracellular compartment. In this model with transgenic expression of annexin A5 and α-synuclein, the abundance of intracellular inclusion bodies is reduced by annexin A5. Thus, annexin A5 may be associated with the pathogenesis of β-cell deficiency in diabetes mellitus and loss of dopaminergic neurons in Parkinson's disease, and further studies should test this hypothesis.

In conclusion, the data presented here support the concept that annexin A5 protects β-cells from h-IAPP-induced apoptosis by a mechanism involving a direct interaction with h-IAPP and alteration of its aggregation pathway. The in vivo model (*C. elegans*) with transgenic expression of α-synuclein and annexin A5 extends the relevance of this finding since this mechanism is also operative with endogenous expression of annexin A5 and another amyloidogenic protein. Therefore, it is interesting to speculate that at least some members of the annexin family of proteins might play a physiological role in protecting cells from amyloid protein toxicity.

ACKNOWLEDGMENT

Human islets of Langerhans for confocal microscopy were provided by the Cell Isolation and Transplantation Center at the University of Geneva School of Medicine, thanks to the ECIT "islets for research" distribution program sponsored by the Juvenile Diabetes Research Foundation. Human pancreatic islets for static incubation experiments were provided by the Diabetes

Institute for Immunology and Transplantation, University of Minnesota, and the Northwest Tissue Center. We also thank Bridget LaMonica for making the *C. elegans* strains and lysates.

REFERENCES

1. Janson, J., Ashley, R. H., Harrison, D., McIntyre, S., and Butler, P. C. (1999) The mechanism of islet amyloid polypeptide toxicity is membrane disruption by intermediate-sized toxic amyloid particles. *Diabetes 48*, 491–498.
2. Lashuel, H. A., Hartley, D., Petre, B. M., Walz, T., and Lansbury, P. T., Jr. (2002) Neurodegenerative disease: Amyloid pores from pathogenic mutations. *Nature 418*, 291.
3. Bates, G. (2003) Huntingtin aggregation and toxicity in Huntington's disease. *Lancet 361*, 1642–1644.
4. Glabe, C. G., and Kayed, R. (2006) Common structure and toxic function of amyloid oligomers implies a common mechanism of pathogenesis. *Neurology 66*, S74–S78.
5. Lansbury, P. T., and Lashuel, H. A. (2006) A century-old debate on protein aggregation and neurodegeneration enters the clinic. *Nature 443*, 774–779.
6. Jayasinghe, S. A., and Langen, R. (2007) Membrane interaction of islet amyloid polypeptide. *Biochim. Biophys. Acta 6*, 6.
7. Kayed, R., Head, E., Thompson, J. L., McIntire, T. M., Milton, S. C., Cotman, C. W., and Glabe, C. G. (2003) Common structure of soluble amyloid oligomers implies common mechanism of pathogenesis. *Science 300*, 486–489.
8. Huang, C. J., Lin, C. Y., Haataja, L., Gurlo, T., Butler, A. E., Rizza, R. A., and Butler, P. C. (2007) High expression rates of human islet amyloid polypeptide induce endoplasmic reticulum stress mediated β-cell apoptosis, a characteristic of humans with type 2 but not type 1 diabetes. *Diabetes 56*, 2016–2027.
9. Anguiano, M., Nowak, R. J., and Lansbury, P. T. Jr. (2002) Protofibrillar islet amyloid polypeptide permeabilizes synthetic vesicles by a pore-like mechanism that may be relevant to type II diabetes. *Biochemistry 41*, 11338–11343.
10. Ritzel, R. A., Meier, J. J., Lin, C. Y., Veldhuis, J. D., and Butler, P. C. (2007) Human islet amyloid polypeptide oligomers disrupt cell coupling, induce apoptosis, and impair insulin secretion in isolated human islets. *Diabetes 56*, 65–71.
11. Luibl, V., Isas, J. M., Kayed, R., Glabe, C. G., Langen, R., and Chen, J. (2006) Drusen deposits associated with aging and age-related macular degeneration contain nonfibrillar amyloid oligomers. *J. Clin. Invest. 116*, 378–385.
12. Maloy, A. L., Longnecker, D. S., and Greenberg, E. R. (1981) The relation of islet amyloid to the clinical type of diabetes. *Hum. Pathol. 12*, 917–922.
13. Clark, A., Wells, C. A., Buley, I. D., Cruickshank, J. K., Vanhegan, R. I., Matthews, D. R., Cooper, G. J., Holman, R. R., and Turner, R. C. (1988) Islet amyloid, increased A-cells, reduced B-cells and exocrine fibrosis: Quantitative changes in the pancreas in type 2 diabetes. *Diabetes Res. 9*, 151–159.
14. Hull, R. L., Westermark, G. T., Westermark, P., and Kahn, S. E. (2004) Islet amyloid: A critical entity in the pathogenesis of type 2 diabetes. *J. Clin. Endocrinol. Metab. 89*, 3629–3643.
15. Butler, A. E., Janson, J., Bonner-Weir, S., Ritzel, R., Rizza, R. A., and Butler, P. C. (2003) β-Cell deficit and increased β-cell apoptosis in humans with type 2 diabetes. *Diabetes 52*, 102–110.
16. Butler, A. E., Jang, J., Gurlo, T., Carty, M. D., Soeller, W. C., and Butler, P. C. (2004) Diabetes due to a progressive defect in β-cell mass in rats transgenic for human islet amyloid polypeptide (HIP Rat): A new model for type 2 diabetes. *Diabetes 53*, 1509–1516.
17. Lorenzo, A., Razzaboni, B., Weir, G. C., and Yankner, B. A. (1994) Pancreatic islet cell toxicity of amylin associated with type-2 diabetes mellitus. *Nature 368*, 756–760.
18. Zhang, S., Liu, J., Saafi, E. L., and Cooper, G. J. (1999) Induction of apoptosis by human amylin in RINm5F islet β-cells is associated with enhanced expression of p53 and p21WAF1/CIP1. *FEBS Lett. 455*, 315–320.
19. Saafi, E. L., Konarkowska, B., Zhang, S., Kistler, J., and Cooper, G. J. (2001) Ultrastructural evidence that apoptosis is the mechanism by which human amylin evokes death in RINm5F pancreatic islet β-cells. *Cell Biol. Int. 25*, 339–350.
20. O'Brien, T. D., Butler, P. C., Kreutter, D. K., Kane, L. A., and Eberhardt, N. L. (1995) Human islet amyloid polypeptide expression in COS-1 cells. A model of intracellular amyloidogenesis. *Am. J. Pathol. 147*, 609–616.
21. Ritzel, R. A., and Butler, P. C. (2003) Replication increases β-cell vulnerability to human islet amyloid polypeptide-induced apoptosis. *Diabetes 52*, 1701–1708.
22. Verchere, C. B., D'Alessio, D. A., Palmiter, R. D., Weir, G. C., Bonner-Weir, S., Baskin, D. G., and Kahn, S. E. (1996) Islet amyloid formation associated with hyperglycemia in transgenic mice with pancreatic β cell expression of human islet amyloid polypeptide. *Proc. Natl. Acad. Sci. U.S.A. 93*, 3492–3496.
23. Janson, J., Soeller, W. C., Roche, P. C., Nelson, R. T., Torchia, A. J., Kreutter, D. K., and Butler, P. C. (1996) Spontaneous diabetes mellitus in transgenic mice expressing human islet amyloid polypeptide. *Proc. Natl. Acad. Sci. U.S.A. 93*, 7283–7288.
24. Iwai, A. (2000) Properties of NACP/α-synuclein and its role in Alzheimer's disease. *Biochim. Biophys. Acta 1502*, 95–109.
25. Kahle, P. J., Neumann, M., Ozmen, L., Muller, V., Jacobsen, H., Schindzielorz, A., Okochi, M., Leimer, U., Putten, H., Probst, A., Kremmer, E., Kretzschmar, H. A., and Haass, C. (2000) Subcellular localization of wild-type and Parkinson's disease-associated mutant α-synuclein in human and transgenic mouse brain. *J. Neurosci. 20*, 6365–6373.
26. Mirzabekov, T. A., Lin, M. C., and Kagan, B. L. (1996) Pore formation by the cytotoxic islet amyloid peptide amylin. *J. Biol. Chem. 271*, 1988–1992.
27. Rescher, U., and Gerke, V. (2004) Annexins: Unique membrane binding proteins with diverse functions. *J. Cell Sci. 117*, 2631–2639.
28. Reutelingsperger, C. P. (2001) Annexins: Key regulators of haemostasis, thrombosis, and apoptosis. *Thromb. Haemostasis 86*, 413–419.
29. Flaherty, M. J., West, S., Heimark, R. L., Fujikawa, K., and Tait, J. F. (1990) Placental anticoagulant protein-I: Measurement in extracellular fluids and cells of the hemostatic system. *J. Lab. Clin. Med. 115*, 174–181.
30. Romisch, J., Schuler, E., Bastian, B., Burger, T., Dunkel, F. G., Schwinn, A., Hartmann, A. A., and Paques, E. P. (1992) Annexins I to VI: Quantitative determination in different human cell types and in plasma after myocardial infarction. *Blood Coagulation Fibrinolysis 3*, 11–17.
31. Huber, R., Romisch, J., and Paques, E. P. (1990) The crystal and molecular structure of human annexin V, an anticoagulant protein that binds to calcium and membranes. *EMBO J. 9*, 3867–3874.
32. Lee, G., Pollard, H. B., and Arispe, N. (2002) Annexin 5 and apolipoprotein E2 protect against Alzheimer's amyloid-β-peptide cytotoxicity by competitive inhibition at a common phosphatidylserine interaction site. *Peptides 23*, 1249–1263.
33. Crabb, J. W., Miyagi, M., Gu, X., Shadrach, K., West, K. A., Sakaguchi, H., Kamei, M., Hasan, A., Yan, L., Rayborn, M. E., Salomon, R. G., and Hollyfield, J. G. (2002) Drusen proteome analysis: An approach to the etiology of age-related macular degeneration. *Proc. Natl. Acad. Sci. U.S.A. 99*, 14682–14687.
34. Schlaepfer, D. D., Jones, J., and Haigler, H. T. (1992) Inhibition of protein kinase C by annexin V. *Biochemistry 31*, 1886–1891.
35. Isas, J. M., Cartailler, J. P., Sokolov, Y., Patel, D. R., Langen, R., Luecke, H., Hall, J. E., and Haigler, H. T. (2000) Annexins V and XII insert into bilayers at mildly acidic pH and form ion channels. *Biochemistry 39*, 3015–3022.
36. Jayasinghe, S. A., and Langen, R. (2004) Identifying structural features of fibrillar islet amyloid polypeptide using site-directed spin labeling. *J. Biol. Chem. 279*, 48420–48425.
37. Chen, M., Margittai, M., Chen, J., and Langen, R. (2007) Investigation of α-synuclein fibril structure by site-directed spin labeling. *J. Biol. Chem. 282*, 24970–24979.
38. Der-Sarkissian, A., Jao, C. C., Chen, J., and Langen, R. (2003) Structural organization of α-synuclein fibrils studied by site-directed spin labeling. *J. Biol. Chem. 278*, 37530–37535.
39. Padrick, S. B., and Miranker, A. D. (2002) Islet amyloid: Phase partitioning and secondary nucleation are central to the mechanism of fibrillogenesis. *Biochemistry 41*, 4694–4703.
40. Torok, M., Milton, S., Kayed, R., Wu, P., McIntire, T., Glabe, C. G., and Langen, R. (2002) Structural and dynamic features of Alzheimer's Aβ peptide in amyloid fibrils studied by site-directed spin labeling. *J. Biol. Chem. 277*, 40810–40815.
41. Margittai, M., and Langen, R. (2004) Template-assisted filament growth by parallel stacking of tau. *Proc. Natl. Acad. Sci. U.S.A. 101*, 10278–10283.
42. Margittai, M., and Langen, R. (2008) Fibrils with parallel in-register structure constitute a major class of amyloid fibrils: Molecular insights from electron paramagnetic resonance spectroscopy. *Q. Rev. Biophys. 41*, 265–297.
43. Hamamichi, S., Rivas, R. N., Knight, A. L., Cao, S., Caldwell, K. A., and Caldwell, G. A. (2008) Hypothesis-based RNAi screening

identifies neuroprotective genes in a Parkinson's disease model. *Proc. Natl. Acad. Sci. U.S.A. 105*, 728–733.
44. van Ham, T. J., Thijssen, K. L., Breitling, R., Hofstra, R. M., Plasterk, R. H., and Nollen, E. A. (2008) *C. elegans* model identifies genetic modifiers of α-synuclein inclusion formation during aging. *PLoS Genet. 4*, e1000027.
45. Giambanco, I., Sorci, G., Antonioli, S., Rambotti, M. G., Spreca, A., Bocchini, V., and Donato, R. (1993) Immunocytochemical analyses of annexin V (CaBP33) in a human-derived glioma cell line. Expression of annexin V depends on cellular growth state. *FEBS Lett. 323*, 45–50.
46. Butler, A. E., Janson, J., Soeller, W. C., and Butler, P. C. (2003) Increased β-cell apoptosis prevents adaptive increase in β-cell mass in mouse model of type 2 diabetes: Evidence for role of islet amyloid formation rather than direct action of amyloid. *Diabetes 52*, 2304–2314.
47. O'Brien, T. D., Butler, A. E., Roche, P. C., Johnson, K. H., and Butler, P. C. (1994) Islet amyloid polypeptide in human insulinomas. Evidence for intracellular amyloidogenesis. *Diabetes 43*, 329–336.
48. Lin, C. Y., Gurlo, T., Kayed, R., Butler, A. E., Haataja, L., Glabe, C. G., and Butler, P. C. (2007) Toxic human islet amyloid polypeptide (h-IAPP) oligomers are intracellular, and vaccination to induce anti-toxic oligomer antibodies does not prevent h-IAPP-induced β-cell apoptosis in h-IAPP transgenic mice. *Diabetes 56*, 1324–1332.